RSC Sustainability

ROYAL SOCIETY OF CHEMISTRY

PAPER

View Article Online
View Journal | View Issue

Cite this: *RSC Sustainability*, 2025, **3**, 5314

Pyrolysis of waste pinewood sawdust using Py-GC-MS: effect of temperature and catalysts on the pyrolytic product composition

Ranjeet Kumar Mishra, *[a] Sampath Chinnam,[b] Naveen Dwivedi[c] and Bishnu Acharya*[d]

Pyrolysis of waste pinewood sawdust (PWS) was investigated using Py-GC-MS to gauge its suitability for generating fuel and chemicals. The experiments were performed from 450–600 °C under purely thermal conditions and in the presence of 10 wt% HZSM-5, CuO and CaO, respectively. TGA revealed a three-stage degradation, with the second stage responsible for roughly 76.50 wt% of mass loss. Furthermore, the inherent inorganic elements in PWS, including Ca, K, Mn, Mg, Si, Fe, Co, Zn, Ba, Na, Sr, Ti, Pb, B, Cu, and Ni, were found to influence the pyrolysis product distribution. FTIR spectra confirmed characteristic C–O, C–H, C=O and O–H bands arising from hemicellulose, cellulose and lignin. Py-GC-MS showed that HZSM-5, CuO, and CaO reduced phenol by 11.79%, 15.78%, and 13.03% respectively, and decreased acid fractions by 6.49%, 7.06%, and 7.33%, respectively. In contrast, these catalysts increased hydrocarbon yields by 5.0%, 6.15%, and 6.72% at 550 °C. The results demonstrated that catalyst selection, temperature control, and inherent mineral content collectively govern product yields, supporting thermo-catalytic pyrolysis as a sustainable route for PWS valorisation into higher-quality fuels. Furthermore, thermo-catalytic pyrolysis emerges as a promising,sustainable route for converting PWS into higher-quality fuel and satisfying the SDGs 7, 9, 12, and 13.

Received 12th August 2025
Accepted 8th September 2025

DOI: 10.1039/d5su00665a

rsc.li/rscsus

Sustainability spotlight

This study demonstrates a sustainable pathway for converting waste pine sawdust into high-value biofuels and chemicals *via* thermo-catalytic pyrolysis. By integrating efficient catalysts such as HZSM-5, CaO, and CuO, the process significantly reduces oxygenates and undesirable acids while enhancing hydrocarbon yields. The use of Py-GC-MS enables precise optimisation of pyrolysis conditions, supporting cleaner, energy-dense fuel alternatives. This approach promotes circular economic principles and aligns with global efforts toward reducing fossil fuel dependency and greenhouse gas emissions through green, waste-to-energy technologies. This study covered United Nations Sustainable Development Goals (SDGs) 7, 12, 13 and 9.

1. Introduction

The annual increase in energy demand is primarily driven by rapid population growth and industrialisation, while the availability of energy sources is either stagnating or declining. Energy plays a crucial role in facilitating human advancement and technological development, serving as the essential input for various sectors, including manufacturing, transportation, and production activities.[1] However, the rate of energy consumption is outpacing energy production, and fossil fuel reserves are on the verge of depletion. Currently, the primary energy sources are petroleum (31.1%), coal (28.9%), and natural gas (21.4%), while green fuels contribute 10.20%. Nuclear energy accounts for 4.8%, hydrothermal energy 2.4%, and renewable sources like solar, wind, and geothermal energy make up a smaller yet growing fraction of the energy mix.[2] The reliance on fossil fuels is resulting in resource exhaustion and escalating greenhouse gas emissions. The diminishing availability of fossil fuels is also a critical factor contributing to the rising costs of petroleum-derived products, including petrol, diesel, and kerosene. Renewable energy sources offer significant environmental benefits due to their much lower emissions compared to fossil fuels. Biomass stands out for its versatility, as it can be converted into solid, liquid, and gaseous forms. Biomass is characterised by its low sulphur, nitrogen, and ash contents, making it an environmentally sustainable option. It is not only carbon-neutral but also has the potential to help

[a]*Department of Chemical Engineering, Manipal Institute of Technology, Manipal Academy of Higher Education, Manipal, Karnataka 576104, India. E-mail: ranjeet.mishra@manipal.edu*

[b]*Department of Chemistry, M. S. Ramaiah Institute of Technology, Bangalore 560 054, Karnataka, India*

[c]*Department of Biotechnology Engineering and Food Technology, University Institute of Engineering, Chandigarh University, Mohali, Punjab 140413, India*

[d]*Department of Chemical and Biological Engineering, University of Saskatchewan, 57 Campus Drive, Saskatoon, SK S7N5A9, Canada. E-mail: bishnu.acharya@usask.ca*

address energy shortages. India, with its abundant forests, wood resources, and agricultural by-products, utilises approximately 500 million metric tons (MMT) of raw biomass annually, according to a survey.[3] Furthermore, energy generation has reached 18 000 MW through the use of 120–150 million metric tons of forestry and agricultural biomass each year.[3] On a global scale, biomass contributes approximately 10–14% to the overall energy supply.[4] Biomass conversion can be accomplished through biochemical and thermochemical processes. The biochemical approach involves techniques such as fermentation, aerobic digestion, and anaerobic digestion, where biomass is decomposed into lower molecular weight substances with the aid of enzymes or bacteria acting as catalysts.[5] This process generally necessitates a longer duration to transform biomass into products of higher value. Conversely, the thermochemical process encompasses methods such as combustion, gasification, pyrolysis, liquefaction, and co-firing. In this context, biomass is broken down into smaller molecular-weight compounds through the application of heat.[6] Notably, pyrolysis is distinguished among thermochemical techniques for its capability to convert biomass into solid, liquid, and gaseous products.[7]

The analytical pyrolysis method (Py-GC-MS) breaks down complex biomass, polymers, and waste into smaller volatile molecules through thermal breakdown. In this method, samples are rapidly heated in an inert atmosphere, typically from 500–900 °C, leading to thermal cracking into volatile compounds.[8] These volatiles are immediately transferred to a gas chromatograph and separated based on their boiling points. The separated compounds are further identified and quantified using a mass spectrometer, which provides precise molecular and structural information. Py-GC-MS enables real-time, in-depth characterisation of pyrolysis products including hydrocarbons, phenols, acids, ketones, and oxygenates. It is especially valuable in catalytic pyrolysis research on waste and polymers, as it enables evaluation of catalyst efficiency in deoxygenating bio-oil vapours and increasing the yield of desirable fuel-range compounds.[9] This technique plays a critical role in optimising pyrolysis conditions for biofuel and chemical production. Catalytic cracking is adopted widely as it has tunable properties, allowing for precise control over the product composition and quality.[10] This process enhances the conversion of complex organic molecules into simpler hydrocarbons, enabling the production of valuable fuels and chemicals.[11,12] The choice of HZSM-5, CuO, and CaO was premeditated to balance proven catalytic performance, commercial availability, and comparability with existing literature for benchmarking. HZSM-5 is slightly costly but highly effective for producing aromatics through acidic cracking. CuO is cheaper and supports redox-driven deoxygenation, while CaO neutralises acids through its basicity. These catalysts follow three different routes: acidic cracking, oxidative upgrading, and base-catalysed deacidification. Therefore, utilising well-documented and inexpensive catalysts enables direct performance comparison with prior studies, ensuring that observed improvements are attributable to process optimisation rather than the novelty of the catalyst. They often lack scale-up readiness, cost-effectiveness, and long-term stability under pyrolysis conditions, while emerging nanostructured or bifunctional catalysts may offer advantages.[13] HZSM-5 (depending on the silica and alumina ratio) facilitates the conversion of biomass into valuable hydrocarbons and aromatic compounds while promoting selective cracking.[14] Furthermore, copper oxide (CuO) enhances the reaction kinetics and aids in the reduction of oxygenated compounds, improving the quality of fuel. Finally, calcium oxide (CaO) helps capture acidic gases and stabilise the pyrolysis products.[15] Mishra *et al.* (2023) studied the pyrolysis of *Azadirachta indica* seeds in a semi-batch reactor using CaO and CuO catalysts. Thermal pyrolysis yielded 39.53 wt% liquid, while adding 20% catalysts increased yields to 46.53 wt% with CaO and 45.36 wt% with CuO. Catalysts notably enhanced pyrolytic oil quality by reducing oxygenated compounds, acids, and phenols, while increasing hydrocarbons, aldehydes, and alcohols.[15] Wang *et al.* (2020) studied the catalytic pyrolysis of cedar wood in a Py-GC-MS analyser using zeolite and reported that the use of a catalyst reduced acetic acid by 65.2% and 23.3% under CaO and Al_2O_3 catalysis, respectively, whereas guaiacols decreased by 40.4% and 27.6%, respectively.[16] Sun *et al.* (2015) examined the catalytic pyrolysis of wood sawdust using Fe/CaO catalysts *via* Py-GC-MS and found that the impregnated Fe/CaO (im-Fe/CaO) catalyst outperformed the mechanically mixed Fe/CaO (mix-Fe/CaO) in enhancing bio-oil quality. The im-Fe/CaO catalyst more effectively reduced oxygenated compounds, including acids, aldehydes, and ketones, converting them into a wider range of hydrocarbons.[17] Rahman *et al.* (2020) investigated the catalytic pyrolysis of pinewood over ZSM-5 and CaO using Py-GC-MS for aromatic hydrocarbon production. ZSM-5 exhibited superior catalytic activity, with aromatic yields increasing alongside higher ZSM-5 loadings, reaching a maximum of 42.19 wt% at a biomass-to-catalyst ratio of 0.25 : 1. In contrast, CaO was not selective for aromatic hydrocarbon formation but showed strong deacidification of pyrolytic vapours compared to ZSM-5. Furthermore, non-catalytic pyrolysis produced significantly higher acidic species (13.45 wt%) and phenolics (46.50 wt%).[18] Fang *et al.* (2020) investigated the pyrolysis of poplar sawdust using Fe/Zn-modified ZSM-5 in a Py-GC-MS system. Fe-modified ZSM-5 achieved the highest phenol yield, 18.30% higher than that of pure ZSM-5. Single-metal-supported catalysts with Fe or Zn produced the lowest acid yields, 50.66% lower than that in direct pyrolysis. Metal modification significantly enhanced aromatic hydrocarbon production; however, Fe–Zn co-modified ZSM-5 showed the weakest aromatic promotion among the catalysts, though it still achieved a 68.50% increase compared to direct pyrolysis.[19] Chaihad *et al.* (2021) investigated catalytic pyrolysis of sunflower stalks over bifunctional Cu-loaded HZSM-5 and found that low Cu loadings maintained the crystalline framework and acidity of HZSM-5. The catalyst with 0.5 wt% Cu achieved the best performance, producing 73.2% relative aromatic hydrocarbons and a specific aromatic yield of 56.5 mg per g biomass (d.a.f), significantly outperforming the parent HZSM-5, which yielded 55.0% and 26.0 mg g^{-1}-biomass, respectively.[20] Santos *et al.* (2024) examined the pyrolysis of brewer's spent grain for fuel production. Their research

revealed that catalytic processes yielded only a marginal increase in oil output compared to non-catalytic methods; however, the application of CaO significantly improved the quality of the oil by increasing hydrocarbon levels and facilitating deoxygenation.[21] Singh *et al.* (2023) conducted a study on the catalytic pyrolysis of sawdust pellets using MgO, CuO, Bi_2O_3, NiO, and ZnO, within an Al_2O_3 fixed-bed reactor. They reported achieving a maximum oil yield of approximately 39% at 550 °C under non-catalytic conditions. The composition of the pyrolytic oil varied depending on the metal oxides, resulting in a higher phenolic content (~58%). Additionally, increasing the loading of MgO (from 5 to 20 wt%) and adjusting the catalyst-to-biomass ratios (1 : 1) led to enhanced hydrocarbon yields of approximately 15%.[22] Li *et al.* (2023) explored the pyrolysis of green templates, specifically cellulose, starch, and glucose, using HZSM-5. The results demonstrated exceptional catalytic performance, achieving a maximum yield of BTX compounds at 10.18 wt%, which was approximately 1.1 times greater than that obtained with HZSM-5 alone.[23]

Although the pyrolysis of biomass has been explored, there is still a great deal to study about the specific effects of different catalysts on the distribution and quality of the final product. PWS is a distinctive feedstock owing to its high cellulose (49.54%), hemicellulose (22.14%), and moderate lignin (9.11%) contents, which makes it highly suitable for producing bio-oil and hydrocarbons. Moreover, pinewood sawdust (PWS) is abundantly available in southern India and holds significant potential for bioenergy production. Unlike other lignocellulosic wastes, PWS has lower moisture (7.16%) and ash (2.59%), ensuring efficient pyrolysis with lesser energy losses. Furthermore, its inherent mineral composition (Table 2), including calcium (35.02%) and potassium (18.35%), promotes cracking and decarboxylation, which enhances hydrocarbon and gas yields. In addition, transition metals such as Mn (7.20%), Fe (2.0%), and Cu (1.2%) catalyse deoxygenation reactions and help reduce tar formation. Furthermore, the interaction between metals and catalysts (HZSM-5, CuO, and CaO) creates synergistic effects, amplifying deoxygenation and reducing oxygenated compounds like phenols and acids. This mineral–catalyst interaction highlights PWS as a unique and valuable feedstock compared with conventional biomass. Furthermore, limited information is available on the pyrolysis parameters, such as the effect of temperatures (450–600 °C or more) and catalyst-to-biomass ratios on the production of chemicals and fuel. It is possible to address sustainability and feasibility in biomass consumption by thoroughly profiling the pyrolysis products using Py-GC-MS. Therefore, the present study addressed the thermal and catalytic pyrolysis of PWS using a Py-GC-MS analyser to understand the effect of catalysts on product compositions. HZSM-5, CaO, and CuO were used in this study at 10 wt%, and the catalyst loading was selected from recently published literature.[24,25] Furthermore, PWS was thoroughly characterised through its physicochemical properties, including proximate analysis, elemental composition, higher heating value (HHV), and biochemical constituents. Finally, the gas compositions (hot vapours) were analysed using Py-GC-MS to support the candidacy of biomass as a viable bioenergy feedstock.

2. Materials and methods

2.1. Sample collection and preparation

Pinewood sawdust (PWS) was collected from a local wood mill in Tamil Nadu state, India. The collected PWS was sun-dried for over a week and placed in a hot air oven at 105 °C for 24 h to eliminate the moisture content consistently. Furthermore, the PWS was pulverised into powder form (900–100 μm). The particle size of biomass was estimated using screens (mesh-900–700 μm). The powdered sample is stored in an airtight plastic bag for further experiments. The catalyst, HZSM-5 (SiO_2/Al_2O_3 ratio: 26, crystal size: 300 nm, and BET: 362 $m^2\ g^{-1}$) was purchased from Yaavik Materials and Engineering Private Limited, Rajasthan, whereas CaO (BET surface area, 37 $m^2\ g^{-1}$) and CuO (BET surface area, 29 $m^2\ g^{-1}$) were purchased from Thermo Scientific, Mumbai, India. In this study, the catalysts were used without any pretreatment.

2.2. Physicochemical characterisation of biomass

The proximate analysis was carried out in accordance with ASTM standards, where moisture content was evaluated following ASTM E-871, while ash content and volatile matter were assessed using ASTM D1102-84. The ultimate analysis of carbon (C), hydrogen (H), and nitrogen (N) in the biomass was executed utilising a PerkinElmer elemental analyzer (Thermo Scientific Flash 2000). The higher heating values (HHVs) of PWS were measured with an oxygen bomb calorimeter. The structural components of biomass play a significant role in pyrolysis, as each compound decomposes in distinct temperature ranges. Finally, the Van Soest techniques were utilised to analyse the biochemical constituents present in the biomass.[26] The ash content obtained from the proximate analysis facilitated the examination of the mineral content in biomass through an FESEM-EDX analyser. The thermogravimetric profile of PWS was assessed using thermogravimetric analysis (Hitachi, TA-7000) under an inert atmosphere, with PWS heated from 30 to 900 °C at a rate of 10 °C min^{-1} while maintaining a constant inert gas flow rate of 50 mL min^{-1}. Additionally, the functional groups present in PWS were identified using FTIR-ATR (ATR-FTIR, PerkinElmer, Spectrum-two, US), with scanning conducted between 400 and 4000 cm^{-1} at a step size of 4 cm^{-1} and a scanning rate of 128.

2.3. Py-GC/MS

Py-GC/MS was employed to investigate the effect of catalysts (HZSM-5, CuO and CaO at 10 wt% loading) on the pyrolysis vapours from pinewood sawdust. The pyro probe, an advanced analytical tool that integrates a pyrolyzer with a GC/MS, was utilised due to its frequent application in studying the impact of various biomass–catalyst mixtures during catalytic fast pyrolysis. This setup allows for a rapid assessment of pyrolysis products, which was crucial given the lack of existing literature on the use of catalysts in fast pyrolysis. In this investigation, a CDS Pyroprobe 5000 series (CDS Analytical, Inc.) was utilised in conjunction with a GC/MS system (6890 N Network GC System, 5975B inert XL MSD, Agilent Technologies) featuring

a 60 m VF-1701 ms (0.25 μm) column (Agilent J&W Technologies). Approximately 2.45 μg of PWS was introduced into a quartz tube, with small quantities of quartz wool positioned at both ends to facilitate the non-catalytic pyrolysis process. The weight of the sample was measured using a microbalance with a precision of 1 μg. To assess the influence of the catalyst, the PWS was physically blended with the catalyst at a loading ratio of 10 wt%. This mixture was similarly placed in a quartz tube, supported by quartz wool at both ends. The pyrolysis was executed at a heating rate of 20 °C ms^{-1}, reaching a temperature from 450–600 °C. The resulting pyrolysis vapours were swiftly combined with the helium carrier gas in the pyrolyzer interface before being directed to the GC/MS for analysis. The oven temperature commenced at 40 °C for 5 min, subsequently increasing at a rate of 3 °C min^{-1} to 280 °C, where it was maintained isothermally for 10 min. Helium served as a carrier gas, pumped at a flow rate of 1.2 mL min^{-1} in a split mode of 100 : 1. The GC/MS interface was kept at a stable temperature of 300 °C. At the same time, the ion source and auxiliary heater of the mass spectrometer were set at 230 °C and 270 °C, respectively. The GC/MS was operated in electron ionization (EI) mode. To ensure consistency, the experiments were replicated twice. The identification of compounds generated from thermal and catalytic pyrolysis was accomplished by comparing the mass spectra of chromatographic peaks with standard spectra from the National Institute of Standards and Technology (NIST) library. Based on a first-order approximation, the area percentages of chromatographic peaks were presumed to directly correlate with the concentrations of volatile compounds, as the PWS quantity remained unchanged.

3. Results and discussion

3.1. Physicochemical analysis of feedstock

The physicochemical characterisation of PWS, along with wood sawdust,[27] deodar wood sawdust,[28] and corn cob,[29] is presented in Table 1. The proximate study of PWS confirmed 7.16% moisture content, which is found to be within the permissible limits (<10%). Biomass with a moisture content of less than 10% is regarded as the ideal feedstock for pyrolysis and combustion processes.[30] Moisture content plays a crucial role in biomass pyrolysis, which affects efficiency and product distribution. Higher moisture content in biomass decreases the overall thermal efficiency of the process, as additional energy is needed to evaporate the water. This results in lower bio-oil yields and a higher production of water and non-condensable gases. It also prolongs the reaction time and affects the formation of valuable compounds. Ideally, biomass should have a moisture content below 10% to ensure optimal pyrolysis performance, as lower moisture levels enhance bio-oil quality, increase hydrocarbon production, and improve overall process efficiency.[30] The volatile matter of PWS was found to be 74.22 wt%, which is very close to that of wood sawdust (73.40%) but lower than that of deodar wood sawdust (80.87%) and corn cob (80%), respectively. Furthermore, the ash content of PWs was found to be 2.59%, which is well aligned with that of deodar wood sawdust (3.38%) but lower than that of wood sawdust (5.20%) and corn cob (5.70%), respectively. Volatile matter and ash content significantly influence biomass pyrolysis outcomes by affecting product yields and overall process efficiency.[31] Biomass with highly volatile matter produces more bio-oil and gases as volatiles decompose rapidly into smaller, combustible compounds under heat. This leads to increased bio-oil yields, which is beneficial for liquid fuel production. In contrast, biomass with low volatile matter tends to generate more biochar, which can be advantageous for carbon-rich materials but limits bio-oil output.[31] Furthermore, ash content, mainly composed of inorganic minerals such as silica, calcium, and potassium, negatively impacts the pyrolysis process (Table 2).[32] Higher ash content can interfere with heat transfer, causing uneven thermal distribution and reducing the efficiency of biomass conversion. It also promotes undesirable side reactions, potentially lowering bio-oil quality by increasing the formation of oxygenated compounds. Furthermore, ash content

Table 1 Physicochemical characterisation of pinewood sawdust

Analysis	PWS	Wood sawdust[27]	Deodar wood sawdust[28]	Corn cob[29]
Proximate analysis (wt%) dry basis				
Moisture content	7.16 ± 1.20	6.70	3.07	10.2
Volatile matter	74.22 ± 1.41	73.40	80.87	80.0
Ash content	2.59 ± 1.13	5.20	3.38	5.70
Fixed carbon	16.03 ± 1.63	14.70	12.68	4.20
Ultimate analysis (wt%) dry basis				
C	48.31	40.30	46.09	44.20
H	6.50	5.37	7.02	5.90
O	44.51	53.05	46.39	44.20
N	0.68	1.28	0.50	0.54
S	—	—	—	0.08
Heating value (MJ kg^{-1})	18.21 ± 1.12	18.24	18.68	15.50
Chemical analysis (wt%)				
Hemicellulose (HC)	22.14	—	—	29.0
Cellulose (C)	49.54	—	—	32.2
Lignin (L_g)	9.11	—	—	15.8

Table 2 Chemical composition of ash (dry basis wt%) using EDX

Element	Percentage (wt%)
Ca	35.02
K	18.35
Mn	7.20
Mg	5.40
Si	11.20
S	3.30
Al	5.60
Fe	2.00
P	1.10
Co	1.40
Zn	2.80
Ba	1.60
Na	1.20
Sr	0.20
Ti	1.60
Pb	0.20
B	0.60
Cu	1.20
Ni	0.03

can foul reactors and deactivate catalysts, requiring more frequent maintenance and reducing overall process effectiveness.[31] Overall, biomass with lower ash and high volatile content is preferred for efficient pyrolysis. Fixed carbon plays a vital role in biomass pyrolysis by contributing to char production and enhancing the energy content of materials. A higher fixed carbon content increases biochar yield, which is valuable for biochar applications, making it suitable for energy generation. The fixed carbon of PWS was found to be 16.30%, which is slightly higher than that of the other reported biomass in Table 1. The elemental analysis of PWS confirmed 48.31% carbon, 6.50% hydrogen, 44.51% oxygen and 0.68% nitrogen contents. The carbon content of PWS was found to be higher than that of other reported biomass in Table 1, whereas the hydrogen content was found to be within an analogous range. Higher carbon and hydrogen contents in biomass enhance pyrolysis by increasing char and hydrocarbon yields, improving bio-oil quality, and boosting the calorific value for more efficient fuel and energy production.[33] Furthermore, lower nitrogen levels suggest reduced NO_x formation during pyrolysis. The HHV of PWS was found to be 18.21 MJ kg^{-1}, which is aligned with that of wood sawdust and deodar wood sawdust. Biomass with a higher HHV produces more heat and energy during pyrolysis, enhancing the yield and quality of bio-oil, syngas, and char for energy applications.[33] Chemical analysis of PWS revealed a high cellulose content (49.54%) and significant hemicellulose content (22.14%), indicating its strong potential for enhanced liquid yield during pyrolysis due to the thermal decomposition behaviour of these polysaccharides. Finally, 9.11% lignin content in PWS confirms the formation of aromatic derivatives and the formation of char. The elemental composition of ash obtained for PWS confirmed 35.02% Ca, 18.35% K, 7.20 Mn, 5.40 Mg, 11.20 Si, 3.30 S, 5.60 Al and 2% Fe, respectively. During biomass pyrolysis, minerals such as calcium (Ca), potassium (K), manganese (Mn), magnesium (Mg), silicon (Si), sulphur (S), aluminium (Al), and iron (Fe) play critical roles (Py-GC-MS result). These minerals can influence thermochemical processes, affecting the yield and composition of pyrolysis products. For instance, alkaline metals like K and Ca can enhance catalytic activity, promoting the formation of bio-oil and gases. In contrast, transition metals like Fe and Mn may affect char characteristics and reduce tar formation. Additionally, minerals can impact the ash content and combustion properties of the resulting biochar.[34] The specific metal element has a particular effect on the pyrolysis composition. For example, alkali metals like Ca, K, and Na act as catalysts, enhancing the cracking of biomass and promoting the formation of gases and biochar at the expense of bio-oil yield.[35] Furthermore, Mg and Sr similarly facilitate depolymerisation but with milder effects.[36] Transition metals such as Mn, Fe, Co, Ni, and Cu catalyse dehydration, decarboxylation, and demethanation reactions, leading to higher gas-phase yields and modified char structures.[37,38] In addition, Al, Ti, and Si often form inert phases that influence heat transfer without directly catalysing reactions.[39] Heavy metals like Pb and Ba may pose environmental risks by concentrating on the char or bio-oil.[40] Elements such as P and S contribute to the formation of phosphates and sulphides, which may influence the ash composition and catalytic activity during pyrolysis. Trace metals like Zn and B can further affect secondary reactions, modifying tar formation and stability.[40] Overall, the metal content alters reaction pathways, necessitating process optimisation to mitigate adverse effects, such as ash fouling and toxic emissions, while leveraging catalytic benefits for improved product quality and yield.

3.2. FTIR analysis

FTIR analysis is essential for biomass characterisation as it identifies functional groups (–OH, C–H, and C=O) and determines the chemical composition of hemicellulose, cellulose, and lignin. This insight into molecular structures aids in understanding thermal decomposition behaviour and optimising conversion processes like pyrolysis or gasification for bioenergy applications. The spectra depicting wavenumber against transmittance for PWS are presented in Fig. 1. A peak at 3444 cm^{-1} signifies the intermolecular bonding of hydroxyl groups, underscoring the prevalence of OH and N–H groups, which indicates the presence of phenolic, alcoholic, and carboxylic functional groups.[41] The band observed at 2642 cm^{-1} is linked to alkanes and alkenes, corresponding to C–H and = C–H stretching vibrations.[15] Peaks within the range of 1749 to 1638 cm^{-1} are associated with C=O, O–H and C–O stretching in unconjugated ketone carbonyl and the aliphatic xylan group.[42] The bands at 1364 and 1230 cm^{-1} are related to C–H, C–C, C= O, and C=C stretching, indicating the presence of cellulose and hemicellulose.[42] The peak at 1029 cm^{-1}, which corresponds to C–O stretching vibrations, further confirms the presence of cellulose, hemicellulose, and lignin in the biomass.[41] Lastly, the IR band at 662 cm^{-1} attributed to C–H plan, which corroborates the existence of aromatic compounds within the biomass.[41]

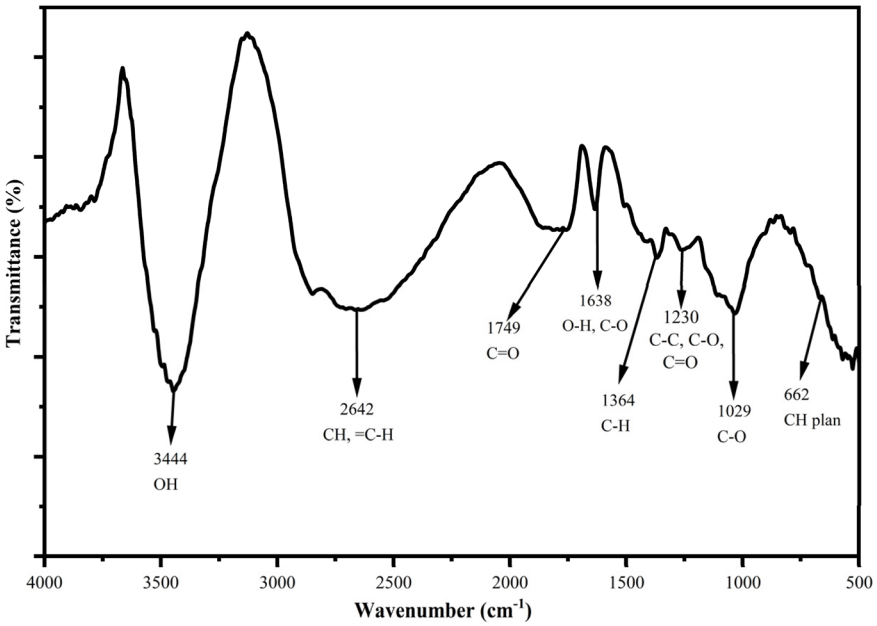

Fig. 1 FTIR analysis of PWS.

3.3. Thermal analysis

The thermal decomposition characteristics of PWS were examined through thermogravimetric analysis (TGA) conducted under non-isothermal conditions. The thermogravimetric profile (Fig. 2) indicated that the decomposition of biomass occurs in three distinct phases: drying (up to 150 °C), devolatilization (150–550 °C), and char formation (>550 °C). It was noted that the elimination of water and low molecular weight substances took place up to 150 °C (Fig. 2). In the 2nd phase, which encompasses temperatures from 150 to 550 °C, the highest level of decomposition was observed (76.52%), primarily attributed to the degradation of hemicellulose and cellulose. The 2nd phase, termed the active pyrolytic zone, is marked by the continuous application of heat, which leads to the fragmentation of higher molecular-weight compounds into lower molecular-weight ones. During this phase, two exothermic reactions occur concurrently, resulting in the

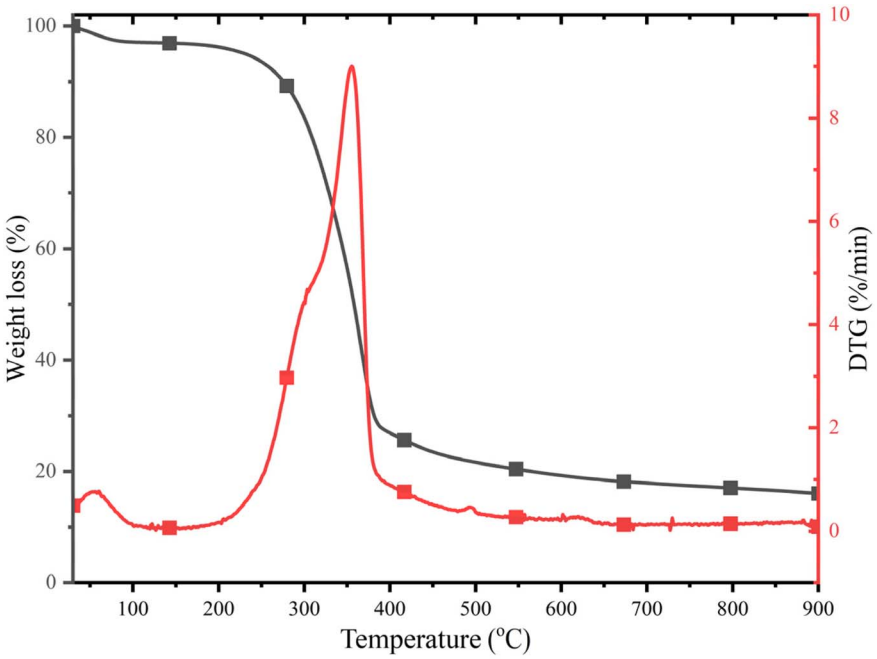

Fig. 2 Thermal stability profile of PWS at a 10 °C per min heating rate.

breakdown of hemicellulose, cellulose, and lignin, which contributes to the generation of higher volatiles. The proximate analysis of PWS (volatile matter) was found to align with this range, with minor discrepancies likely due to the nature of the study. The differential thermogravimetric (DTG) curve (Fig. 2) revealed that the initial peak corresponds to the removal of moisture and light volatiles at temperatures up to 150 °C. The decomposition recorded in the first stage (30–150 °C) was 3.12%. The subsequent phase is linked to the degradation of hemicellulose and cellulose, while lignin decomposes at a slower rate, ultimately leading to the production of maximum biochar. In the final stage (>550 °C), a decomposition rate of 4.31% was observed. The PWS decomposition profile is very similar to that of other reported biomass.[43,44]

3.4. Effect of temperature

The distribution of pyrolysis products from PWS is significantly influenced by the temperature. Cellulose and hemicellulose break down at lower temperatures (350–480 °C), and oxygenated chemicals like acids and ketones were found to be predominant.[45] Furthermore, the acids and ketones decrease as a result of secondary reactions; increasing lignin breakdown promotes the synthesis of phenols and furans as the temperature increases to 500–600 °C.[46] From Fig. 3, it was found that pyrolysis products include mainly phenols, hydrocarbons, ketones, acids, aldehydes, alcohols, furans, and others in terms of relative area (%) across 450, 500, 550, and 600 °C, respectively. The results (Fig. 3) showed that at temperatures above 550 and 600 °C, phenols were the dominant products, contributing over 32%. This shows that at higher temperatures, lignin degrades significantly, yielding phenolic chemicals. Lignin breakdown is endothermic and requires high temperatures (500–600 °C), resulting in a rise in phenolic compounds at 550 °C and 600 °C. At 450 and 500 °C, phenolic content decreases, indicating inadequate lignin degradation.[45] Furthermore, the yield of hydrocarbons remains steady and lower at all temperatures (7–11%). This group is most likely caused by secondary reactions of volatiles and thermal cracking of lipids or extractives. The mild increase from 450 °C to 600 °C supports chain scission reactions and deoxygenation processes that occur at higher temperatures (600 °C).[47] Ketone peaks were found to be higher at 450 and 500 °C (11.56 and 9.25%), and then decrease as the temperature increases to 600 °C. These are typically the byproducts of cellulose and hemicellulose breakdown, mainly by ring-opening and rearrangement processes. The decrease at higher temperatures could be attributable to greater degradation of ketones into smaller gases.[48] Furthermore, acid content was found to be decreased on increasing the pyrolysis temperatures. This trend is found due to hemicellulose pyrolysis, which occurs at lower temperatures (180–250 °C) and produces acetic and formic acids. With increasing temperature, low-molecular-weight acids volatilize and decompose into gases, leading to a reduction in their concentrations.[36] The aldehydes gradually increase from 450–550 °C and remain stable. These chemicals are formed during the breakdown of cellulose, particularly through intermediate anhydrosugar routes. Their presence at mid-range temperatures suggests partial cellulose depolymerisation, while their stability over 600 °C could be owing to saturation of accessible precursor processes. The alcohol production remains minimal, but it steadily increases with increasing pyrolysis temperature. These could result from the cleavage of ether bonds in hemicellulose and lignin, and from hydrogenation processes in the vapour

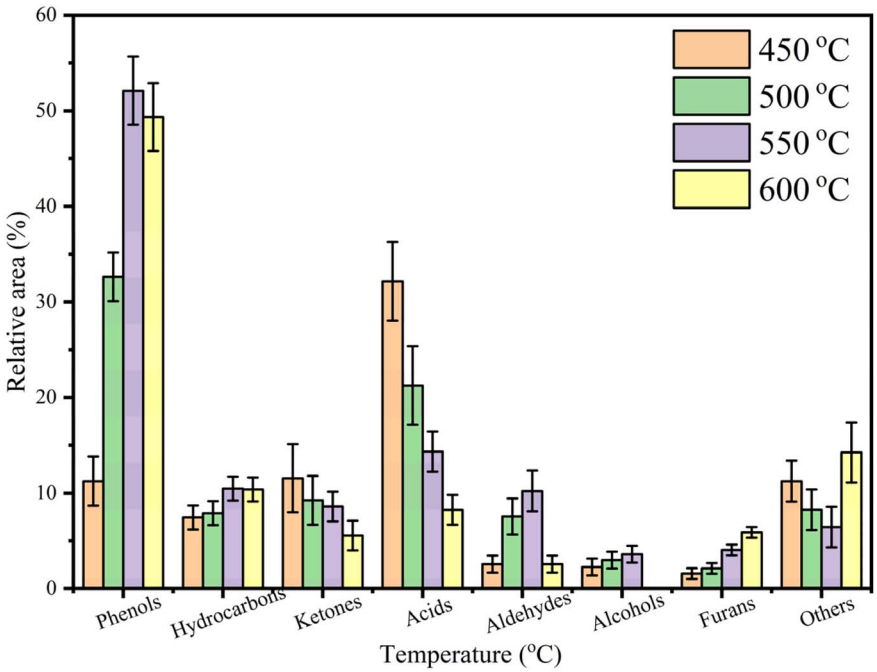

Fig. 3 Effect of pyrolysis temperature on the product compositions.

phase.[45] The increase could be due to radical recombination in the vapour stream with greater energy inputs. The furan compounds formed from the dehydration of pentoses and hexoses increase slowly with temperature. This pattern illustrates the gradual degradation of cellulose and hemicellulose, resulting in furfural and hydroxymethylfurfural (HMF) as intermediates. The increase reflects a shift away from primary pyrolysis and toward secondary ring formation processes, which are more favourable at higher temperatures (550 and 600 °C).[48] Overall, the increasing pyrolysis temperature promotes phenol and furan formation through lignin degradation and secondary reactions, while acids and ketones decrease as cellulose and hemicellulose degrade. Furthermore, the higher temperatures produce aromatic and stable molecules, while lower temperatures produce more oxygenated intermediates, emphasising the significance of temperature management.

3.5. Py-GC-MS analysis

Py-GC/MS analysis of PWS degradation using thermal and catalytic pyrolysis is identified. A pictorial representation is shown in Fig. 4, while the detailed list of compounds is provided in Table S1. The pyrolysis hot vapours mainly consist of phenols, hydrocarbons, ketones, acids, aldehydes, alcohol and furnaces. The temperature selection of PWS was performed from 450–600 °C, whereas the catalyst loading (10 wt%) was selected based on the published literature.[49–51] HZSM-5 effectively produces hydrocarbons in biomass pyrolysis through Brønsted and Lewis acid sites, which catalyse the cracking of larger molecules into smaller molecules. Furthermore, higher acidity enhances conversion efficiency, making zeolites highly effective for improving pyrolysis oil quality by promoting catalytic degradation and hydrocarbon yield during pyrolysis.[52] Py-GC-MS results (Fig. 4) confirmed that thermal pyrolysis of PWS yielded 52.09% phenols, 14.33% acids, 10.48% hydrocarbons, 8.60% ketones, 10.22% aldehydes, 3.60% alcohols, and 4.05% furans. It was noticed that phenol concentration was maximum (52.09%) in PWS pyrolytic vapours due to lignin decomposition. Lignin breaks down into various phenolic derivatives, including phenol, cresols, guaiacol, syringol, catechol, eugenol, vanillin, and syringaldehyde during pyrolysis. These compounds originate from lignin structural units *via* ether and C–C bond cleavage (FTIR analysis), followed by demethoxylation, dealkylation, and oxidation, contributing significantly to the oxygenated fraction of pyrolysis vapours.[53] These phenolics are released as lignin undergoes fragmentation, making them the dominant product during the pyrolysis process.[54] The phenolic results are similar to the results reported for polycarbonate.[54] Aromatic compounds such as benzene, toluene, and xylene are highly valuable in the petrochemical industry.[55] Thermal pyrolysis produces aromatic compounds such as benzene, (1-methylethenyl)-2-phenylpropene, and 1,2,4,5-tetramethylbenzene.[54] The catalytic pyrolysis of PWS at 10 wt% loading produced phenols (40.30, 34.31, and 39.06%), hydrocarbons (15.48, 16.63, and 17.20%), ketones (14.57, 15.43, and 16.33%), acids (7.84, 7.27, and 7.00%), aldehydes (7.05, 11.65, and 10.97%), alcohols (1.93, 1.76, and 1.57%), and furans (2.39, 3.77, and 4.27%) using HZSM-5, CuO, and CaO catalysts, respectively. It was noted that the use of HZSM-5, CuO, and CaO reduces the production of phenolic compounds by promoting deoxygenation and enhancing the breakdown of oxygenated compounds. The

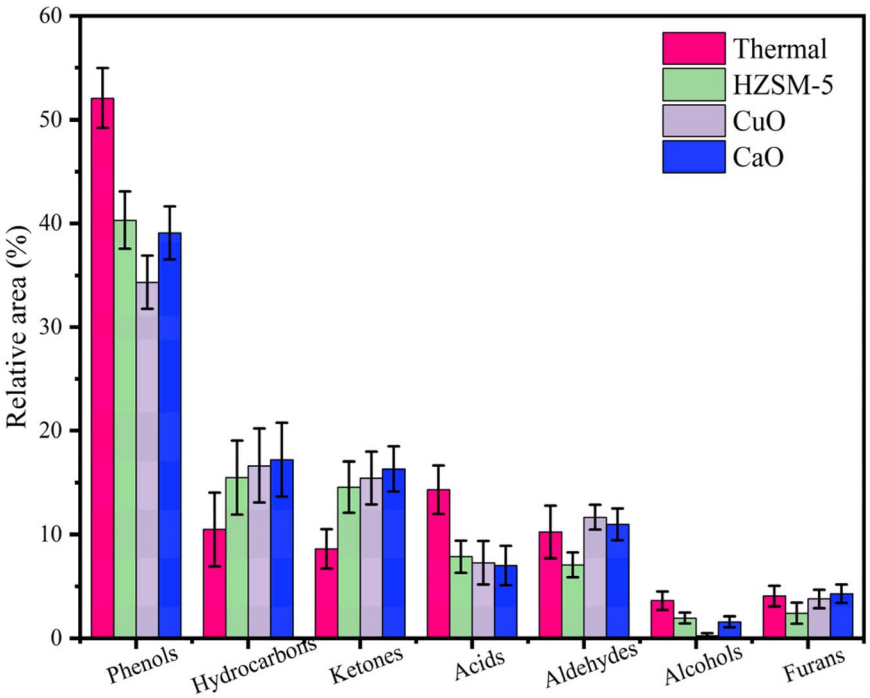

Fig. 4 Py-GC-MS study of thermal and catalytic pyrolysis of PWS at 10 wt% loading.

strong O–H and C=O signals correlate with the high phenolic and acid yields in thermal pyrolysis, as lignin aromatic –OH groups and hemicellulose acetyl groups decompose (FTIR results). Furthermore, HZSM-5 helps break down phenolic compounds into smaller molecules by removing oxygen and cracking their structure. This process changes phenolics into hydrocarbons, mainly aromatics.[56] CuO and CaO assisted by catalysing decarboxylation and dehydrogenation reactions, thus lowering the phenolic content and increasing the yield of hydrocarbons.[57] It was observed that HZSM-5, CuO, and CaO significantly enhance hydrocarbon production. HZSM-5 turns intermediate products into light hydrocarbons due to its high acidity and porous structure.[56] CuO also aids in the deoxygenation of the pyrolysis vapours, while CaO facilitates the removal of acidic compounds.[57] The catalyst significantly reduces acid formation as HZSM-5 acidic sites facilitate conversion of acidic compounds into lighter hydrocarbons, while CuO and CaO endorse deoxygenation and lower or neutralise organic acids.[56] The mineral content present in the sample also influenced the composition of pyrolytic vapours. The higher Ca levels (Table 2) act as natural alkali catalysts, promoting decarboxylation and cracking reactions, which reduce oxygenated compounds and enhance gas and hydrocarbon yields. Furthermore, transition metals like Cu (Table 2) facilitate redox and dehydrogenation reactions, which can improve aromatic and hydrocarbon formation while lowering phenolics through enhanced lignin breakdown. Si and Al influence thermal conductivity and indirectly affect vapour residence time. These inherent minerals may partly mimic the activity of added catalysts, potentially amplifying deoxygenation effects (CaO and CuO), and altering relative yields of phenols, ketones, and hydrocarbons in the Py-GC-MS analysis. The reduction in phenolic and acidic compounds directly influences the chemical compositions and performance of products, enhancing industrial and environmental feasibility. Phenolic compounds are highly reactive due to their hydroxyl functional groups, contributing to polymerisation, oxidative instability, and fouling in industrial processes. Similarly, acidic compounds like carboxylic acids increase the acidity of products, leading to corrosion of processing equipment and storage facilities.[58] By reducing these compounds, the final products exhibit improved thermal and oxidative stability, reduced corrosive behaviour, and an enhanced higher heating value (HHV) in energy applications. From the results, it was noted that CaO is more effective in reducing acids (7.33%) than HZSM-5 (6.49%) and CuO (7.06%), respectively. CaO reacts with carboxylic acids in the pyrolytic vapours, forming stable calcium salts, thus decreasing the acidic content in the bio-oil. This process enhances bio-oil quality by reducing corrosiveness and improving chemical stability for industrial applications.[59] Furthermore, HZSM-5, CuO, and CaO enhance the ketonic compounds (Fig. 4). This synergistic effect increases the yield of ketonic compounds, contributing to improved fuel quality and energy content in the resulting bio-oil.[60] Furthermore, HZSM-5 facilitates the conversion of aldehydes into more stable products, such as hydrocarbons and ketones, through acid-catalysed reactions. Additionally, CuO deoxygenation reduces aldehyde content. Meanwhile, CaO can neutralise acidic species, minimising the conditions conducive to aldehyde formation. This combination results in a lower yield of aldehyde compounds.[61] The alcohol content was also found to be decreased by the incorporation of a catalyst due to the ability to facilitate dehydration and deoxygenation reactions. HZSM-5 converts alcohols into hydrocarbons, CuO aids in oxygen removal, while CaO neutralises acids and facilitates their transformation into more stable, valuable products.[62] Finally, the use of a catalyst reduces the formation of furan compounds primarily due to the catalytic breakdown of hemicellulose, which is a precursor of furans. The functional group C–O stretching in polysaccharides/biopolymers corresponds to ketone and furan formation during cellulose breakdown.[63] The reduction of oxygenated groups in catalytic pyrolysis (FTIR results) matches the lower oxygenate yields and higher hydrocarbon content observed in the Py-GC-MS study. HZSM-5 acidic sites drive dehydration and furan rearrangement into hydrocarbons, while CuO and CaO enhance deoxygenation, converting furan derivatives into stable products and reducing overall furan yield.[62,64]

The product distribution of PWS indicates significant variations in hydrocarbon compositions between thermal and catalytic pyrolysis (HZSM-5, CuO, and CaO) and is presented in Fig. 5. From the results (Fig. 5), it was noted that monocyclic aromatic hydrocarbons (MAHs) dominate, with thermal pyrolysis producing the highest fraction (7.77 wt%), followed closely by CaO (7.28 wt%), while HZSM-5 and CuO show slightly lower yields (6.41–6.69 wt%). The higher MAHs under thermal conditions can be attributed to the absence of catalytic cracking pathways that might instead channel intermediates into polycyclic or other hydrocarbon forms. Furthermore, HZSM-5 convert secondary cyclisation and aromatisation reactions, which produce MAHs, and increases polycyclic aromatic hydrocarbons (PAHs) compared to thermal conditions.[65,66] The formation of PAHs is minimal in thermal pyrolysis (0.37 wt%) but increases significantly with all catalysts (1.35–1.56 wt%), likely due to enhanced aromatic ring growth on catalyst surfaces. The variation of PAHs is attributed to the enhanced deoxygenation, oligomerisation, and cyclisation on catalyst surfaces. Acidic, redox, and basic sites convert oxygenates to reactive intermediates, which undergo aromatic ring growth and condensation, increasing fused-ring PAH formation compared to non-catalytic conditions.[65] The linear hydrocarbons (LHC) are negligible in thermal runs but increase (2.37–2.48 wt%) with catalysts, suggesting that catalytic cracking of heavier molecules generates more open-chain products. This increase results from catalytic cracking of heavy oxygenates and lignin-derived oligomers into open-chain alkanes/alkenes. HZSM-5endorse β-scission and alkyl cracking, CuO redox activity facilitates C–C bond cleavage during deoxygenation, and CaO basic sites drive decarboxylation of fatty acid derivatives, yielding long-chain alkanes such as tricosane. These pathways divert part of the vapour stream from aromatisation, explaining the LHC enhancement.[67] The cyclic hydrocarbons (CHC) are consistently higher in catalytic runs, with CuO giving the maximum (3.91 wt%), slightly above that under thermal conditions (3.87 wt%), and HZSM-5 giving the lowest among the

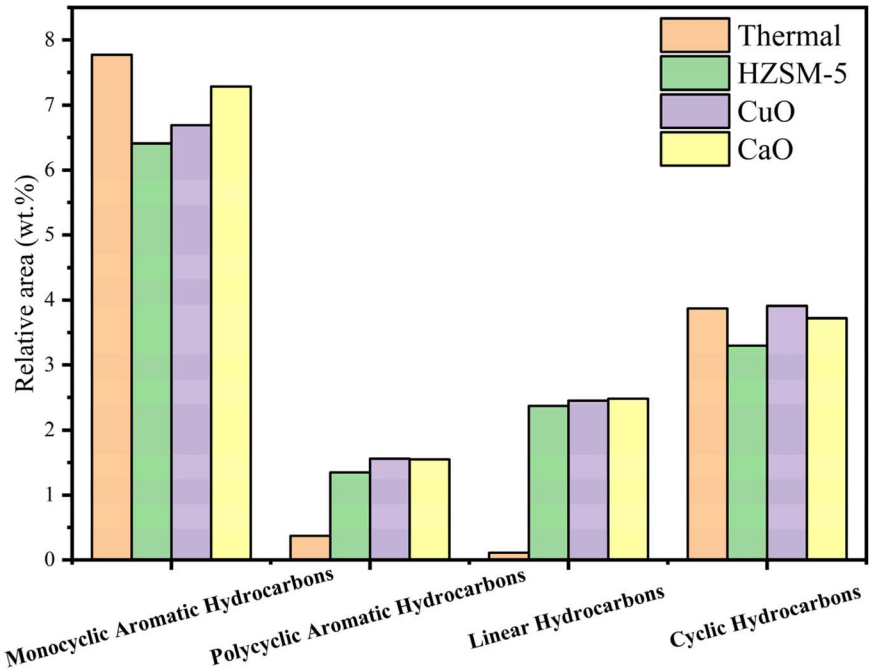

Fig. 5 Distribution of different types of hydrocarbons against the catalyst.

catalysts (3.30 wt%), possibly due to preferential conversion of cyclic intermediates into aromatics.[68] Overall, catalysts shift product profiles toward greater diversity, enhancing PAHs, and linear, and cyclic hydrocarbons while moderating MAHs, driven by their specific acid–base and redox functionalities. The obtained results have good agreement with the published studies by Wang *et al.* (2020) and Liu *et al.* (2022).[69,70]

4. Limitations of the present study

HZSM-5, CaO and CuO catalysts face significant limitations that affect their industrial utility, as well as the quality of the products derived from their application.[71] HZSM-5 excels in hydrocarbon cracking and aromatisation but suffers from rapid deactivation due to coke deposition (one of the major issues), which necessitates frequent regeneration and increases operational costs.[71] Its micropores can also restrict the conversion of bulky feedstocks, limiting its versatility. Furthermore, CaO is widely used in transesterification and CO_2 adsorption due to its strong basicity. It is highly reactive, making it prone to deactivation through hydration or carbonation in humid environments. Its thermal stability is also limited, and its mechanical integrity is compromised during repeated use, causing catalyst attrition and loss of efficiency.[14] Furthermore, CuO, favoured for redox reactions and bio-oil/hot vapour upgrading, is sensitive to sintering under high-temperature conditions and poisoning by sulphur or halogenated compounds, which diminishes its long-term activity.[14] These challenges necessitate feedstock purification, tailored reaction conditions, and advanced catalyst supports or modifications to improve stability and reusability. Moreover, products derived from used catalysts may require post-treatment to ensure compatibility with industrial standards and environmental regulations, particularly in reducing the aromatic or oxygenate content for cleaner applications.

The major limitation of the present study lies in its laboratory-scale setup, which may not fully replicate the complex conditions of industrial pyrolysis systems, such as varied heat and mass transfer rates, longer vapour residence times, *etc.* Furthermore, the use of a fixed catalyst loading (10 wt%) may restrict understanding of catalyst loading performance relationships. The catalyst optimisation at the analytical stage is still missing in the literature. This study is also lacking in terms of bifunctional, hierarchical, or nanostructured tested catalysts, limiting comparative insights. The reliance on Py-GC-MS provides detailed chemical profiling but is constrained by short residence times and small sample sizes, which may underrepresent secondary reactions prominent at scale. Additionally, the study focuses on compositional analysis without addressing catalyst stability, regeneration, or potential deactivation mechanisms, which are critical for practical application (it is very complex at the analytical stage).

5. Conclusions

The present study demonstrated thermal and catalytic pyrolysis of PWS using HZSM-5, CuO, and CaO. The results confirmed that the introduction of catalysts significantly alters product distribution compared to thermal pyrolysis, enhancing hydrocarbon formation while reducing oxygenated compounds such as acids and phenols. HZSM-5 cracking, aromatisation, and cyclisation lead to higher yields of monocyclic aromatic hydrocarbons. CuO favoured polycyclic aromatic hydrocarbon (PAH) formation *via* redox and deoxygenation pathways, while

increasing overall hydrocarbon content. CaO effectively neutralised acidic vapours and facilitated decarboxylation, resulting in prominent increases in linear hydrocarbon yields. The results confirm these shifts, with hydrocarbons increasing from 10.48 wt% (thermal) to 15.48–17.20 wt% (catalytic) and acids dropping from 14.33 wt% to around 7 wt%. Although PAH levels increased slightly, the overall quality improved through higher energy-dense hydrocarbon content and reduced corrosive oxygenates. The results align with established catalytic mechanisms, confirming the role of acid, redox, and basic sites in steering vapour-phase transformations. Further work is needed to optimise catalyst loading, investigate long-term stability, and test under continuous flow or industrial-scale conditions to validate scalability. Thus, the present study reinforces the potential of HZSM-5, CuO, and CaO for improving fuel quality.

Author contributions

Ranjeet Kumar Mishra: data collection, sample preparation and experimentation, conceptualisation, data curation, methodology, software, investigation, visualisation, writing-original draft, and supervision. Sampath Chinnam and Naveen Dwivedi: data curation, methodology, software, investigation, visualisation, writing-original draft. Bishnu Acharya: data curation, methodology, software, investigation, visualisation, supervision.

Conflicts of interest

The authors announce that they have no known competing financial interests or personal relationships that could have appeared to influence the work presented in this paper.

Data availability

The datasets generated during and/or analysed during the current study are available from the corresponding author upon reasonable request.

Supplementary information is available: the supplemenrty data contains GC-MS analysis. See DOI: **https://doi.org/10.1039/d5su00665a**.

Acknowledgements

The authors have no relevant financial or non-financial interests to disclose. The authors would like to thank Biomass, Bioenergy and Bioproducts Lab, Department of Chemical Engineering, Manipal Institute of Technology, Manipal, and Sophisticated Analytical Instrument Facility (SAIF), IIT Bombay, India, for providing the necessary facilities to carry out the research.

References

1 F. Chien, L. Huang and W. Zhao, *J. Innov. Knowl.*, 2023, **8**, 100298.
2 H. Ritchie, M. Roser and P. Rosado, published online at OurWorldinData.org., 2020, **https://ourworldindata.org/renewable-energy**.
3 N. Singh, A. Kumar and S. Rai, *Renew. Sustain. Energy Rev.*, 2014, **39**, 65–78.
4 L. R. Amjith and B. Bavanish, *Chemosphere*, 2022, **293**, 133579.
5 S. Jha, S. Nanda, B. Acharya and A. K. Dalai, *Energies*, 2022, **15**, 6352.
6 S. Li, X. Chen, A. Liu, L. Wang and G. Yu, *Bioresour. Technol.*, 2015, **179**, 414–420.
7 Y. Zhang, Y. Liang, S. Li, Y. Yuan, D. Zhang, Y. Wu, H. Xie, K. Brindhadevi, A. Pugazhendhi and C. Xia, *Fuel*, 2023, **347**, 128461.
8 H. El Bari, C. K. Fanezoune, B. Dorneanu, H. Arellano-Garcia, T. Majozi, Y. Elhenawy, O. Bayssi, A. Hirt, J. Peixinho, A. Dhahak, M. A. Gadalla, N. H. Khashaba and F. H. Ashour, *J. Anal. Appl. Pyrolysis*, 2024, **178**, 106390.
9 A. Nanduri, S. S. Kulkarni and P. L. Mills, *Renew. Sustain. Energy Rev.*, 2021, **148**, 111262.
10 M. Tawalbeh, A. Al-Othman, T. Salamah, M. Alkasrawi, R. Martis and Z. A. El-Rub, *J. Environ. Manage.*, 2021, **299**, 113597.
11 O. Norouzi, S. Taghavi, P. Arku, S. Jafarian, M. Signoretto and A. Dutta, *J. Anal. Appl. Pyrolysis*, 2021, **158**, 105280.
12 E. Blanquet and P. T. Williams, *J. Anal. Appl. Pyrolysis*, 2021, **159**, 105325.
13 A. Shafizadeh, H. Rastegari, H. Shahbeik, H. Mobli, J. Pan, W. Peng, G. Li, M. Tabatabaei and M. Aghbashlo, *J. Clean. Prod.*, 2023, **400**, 136705.
14 Q. Liu, J. Wang, J. Zhou, Z. Yu and K. Wang, *J. Anal. Appl. Pyrolysis*, 2021, **153**, 104964.
15 R. K. Mishra, R. Saini, D. J. P. Kumar, R. Sankannavar, P. Binnal, N. Dwivedi and P. Kumar, *J. Energy Inst.*, 2023, **111**, 101366.
16 J. Wang, Q. Liu, J. Zhou and Z. Yu, *Waste Biomass Valori.*, 2021, **12**, 3049–3057.
17 L. Sun, X. Zhang, L. Chen, X. Xie, S. Yang, B. Zhao and H. Si, *J. Anal. Appl. Pyrolysis*, 2015, **116**, 183–189.
18 M. M. Rahman, M. Chai, M. Sarker, Nishu and R. Liu, *J. Energy Inst.*, 2020, **93**, 425–435.
19 S. Fang, C. Shi, L. Jiang, P. Li, J. Bai and C. Chang, *Int. J. Energy Res.*, 2020, **44**, 5455–5467.
20 N. Chaihad, A. Anniwaer, S. Karnjanakom, Y. Kasai, S. Kongparakul, C. Samart, P. Reubroycharoen, A. Abudula and G. Guan, *J. Anal. Appl. Pyrolysis*, 2021, **155**, 105079.
21 G. E. D. S. d. Santos, C. R. Duarte, C. E. Hori and M. A. D. S. Barrozo, *J. Energy Inst.*, 2024, **114**, 101586.
22 R. Singh, N. Chakinala, K. Mohanty and A. G. Chakinala, *J. Environ. Chem. Eng.*, 2023, **11**, 111518.
23 X. Li, J. Sun, S. Shao, J. Yan and Y. Cai, *Renew. Energy*, 2023, **206**, 506–513.
24 B. Zhao, H. Yang, H. Zhang, C. Zhong, J. Wang, D. Zhu, H. Guan, L. Sun, S. Yang, L. Chen and H. Xie, *J. Anal. Appl. Pyrolysis*, 2021, **157**, 105227.
25 R. French and S. Czernik, *Fuel Process. Technol.*, 2010, **91**, 25–32.

26 P. v. Soest and R. Wine, *J. Assoc. Off. Anal. Chem.*, 1967, **50**, 50–55.
27 Y. Elhenawy, K. Fouad, M. Bassyouni, O. A. Al-Qabandi and T. Majozi, *Energy Convers. Manage.:X*, 2024, **22**, 100583.
28 A. K. Varma, L. S. Thakur, R. Shankar and P. Mondal, *Waste Manage.*, 2019, **89**, 224–235.
29 T. Raj, M. Kapoor, R. Gaur, J. Christopher, B. Lamba, D. K. Tuli and R. Kumar, *Energy Fuels*, 2015, **29**, 3111–3118.
30 M. S. Ahmad, M. A. Mehmood, O. S. Al Ayed, G. Ye, H. Luo, M. Ibrahim, U. Rashid, I. A. Nehdi and G. Qadir, *Bioresour. Technol.*, 2017, **224**, 708–713.
31 Y. Wang, B. Li, A. Gao, K. Ding, X. Xing, J. Wei, Y. Huang, J. C.-H. Lam, K. Subramanian and S. Zhang, *Fuel*, 2023, **340**, 127496.
32 G. Yildiz, F. Ronsse, R. Venderbosch, R. van Duren, S. R. Kersten and W. Prins, *Appl. Catal., B*, 2015, **168**, 203–211.
33 T. Kar, Ö. Kaygusuz, M. Ş. Güney, E. Cuce, S. Keleş, S. Shaik, A. B. Owolabi, B. E. K. Nsafon, J. M. Ogunsua and J.-S. Huh, *Sustainability*, 2023, **15**, 13718.
34 P. Giudicianni, V. Gargiulo, C. M. Grottola, M. Alfè, A. I. Ferreiro, M. A. A. Mendes, M. Fagnano and R. Ragucci, *Energy Fuel.*, 2021, **35**, 5407–5478.
35 M. Zhao, M. Z. Memon, G. Ji, X. Yang, A. K. Vuppaladadiyam, Y. Song, A. Raheem, J. Li, W. Wang and H. Zhou, *Renew. Energy*, 2020, **148**, 168–175.
36 S. Zhou, Y. Xue, J. Cai, C. Cui, Z. Ni and Z. Zhou, *Chem. Eng. J.*, 2021, **411**, 128513.
37 J. Chen, K. Zhao, Z. Zhao, F. He, Z. Huang and G. Wei, *Int. J. Hydrogen Energy*, 2019, **44**, 4674–4687.
38 X. Shen, J. Zeng, D. Zhang, F. Wang, Y. Li and W. Yi, *Sci. Total Environ.*, 2020, **704**, 135283.
39 H. Raclavská, A. Corsaro, D. Juchelková, V. Sassmanová and J. Frantík, *Fuel Process. Technol.*, 2015, **131**, 330–337.
40 A. Nzihou, B. Stanmore, N. Lyczko and D. P. Minh, *Energy*, 2019, **170**, 326–337.
41 P. Doshi, G. Srivastava, G. Pathak and M. Dikshit, *Waste Manag.*, 2014, **34**, 1836–1846.
42 M. Traoré, J. Kaal and A. Martínez Cortizas, *Wood Sci. Technol.*, 2018, **52**, 487–504.
43 M. Kumar, S. Upadhyay and P. Mishra, *Bioresour. Technol. Rep.*, 2019, **8**, 100186.
44 M. Kumar, S. Sabbarwal, P. Mishra and S. Upadhyay, *Bioresour. Technol.*, 2019, **279**, 262–270.
45 H. D. Kawale and N. Kishore, *J. Energy Resour. Technol.*, 2020, **142**(8), 082306.
46 A. Selvarajoo and D. Oochit, *Mater. Sci. Energy Technol.*, 2020, **3**, 575–583.
47 H. Li, Y. Wu, Z. Yang, Q. Song, J. Zhang and X. Wang, *Fuel*, 2022, **326**, 125095.
48 Z. Hu, T. Zhou, H. Tian, L. Feng, C. Yao, Y. Yin and D. Chen, *Prog. React. Kinet. Mech.*, 2021, **46**, DOI: **10.1177/14686783211010970**.
49 R. K. Mishra, S. Vijay, S. Soni, B. S. Dhanraj, P. Kumar and K. Mohanty, *J. Energy Inst.*, 2024, **114**, 101651.
50 R. K. Mishra and K. Mohanty, *J. Energy Inst.*, 2021, **94**, 252–262.
51 R. K. Mishra and K. Mohanty, *Fuel*, 2020, **280**, 118594.
52 R. Cai, X. Pei, H. Pan, K. Wan, H. Chen, Z. Zhang and Y. Zhang, *Energy Fuels*, 2020, **34**, 11771–11790.
53 A. Yerrayya, U. Natarajan and R. Vinu, *Chem. Eng. Sci.*, 2019, **207**, 619–630.
54 Y. M. N. Al-Hakami, M. A. Wahab, E. Yildirir and F. Ates, *J. Energy Inst.*, 2024, **113**, 101499.
55 M. Saeedi, B. Malekmohammadi and S. Tajalli, *J. Hazard. Mater. Adv.*, 2024, **16**, 100459.
56 S. Cheng, L. Wei and M. Rabnawaz, *Fuel*, 2018, **223**, 252–260.
57 X. Xue, C. Zhang, D. Xia, Y. Wang, J. Liang and Y. Sun, *Chem. Eng. J.*, 2022, **431**, 134251.
58 D. Sulejmanovic, J. R. Keiser, Y.-F. Su, M. D. Kass, J. R. Ferrell III, M. V. Olarte, J. E. Wade IV and J. Jun, *Sustainability*, 2022, **14**, 11743.
59 H. Li, Y. Wang, N. Zhou, L. Dai, W. Deng, C. Liu, Y. Cheng, Y. Liu, K. Cobb and P. Chen, *J. Clean. Prod.*, 2021, **291**, 125826.
60 X. Chen, S. Li, Y. Lin, S. Gao, J. Liu, Y. Xue and X. Gao, *J. Anal. Appl. Pyrolysis*, 2024, **181**, 106607.
61 X. Guo, H. Yang, T. Wenga, R. Zhang, B. Liu and G. Chen, *Biomass Bioenergy*, 2022, **156**, 106316.
62 Y. Zheng, J. Wang, D. Li, C. Liu, Y. Lu, X. Lin and Z. Zheng, *J. Energy Inst.*, 2021, **97**, 58–72.
63 Z. Zhai and K. J. Edgar, *Biomacromolecules*, 2024, **25**, 2261–2276.
64 A. Eschenbacher, P. Fennell and A. D. Jensen, *Energy Fuels*, 2021, **35**, 18333–18369.
65 Z. Luo, K. Lu, Y. Yang, S. Li and G. Li, *RSC Adv.*, 2019, **9**, 31960–31968.
66 W. H. Gong, in *Recent Perspectives in Pyrolysis Research*, IntechOpen, 2021.
67 S. De, *Hydrocarbon Biorefinery*, 2022, pp. 327–354.
68 Y. Shen, C. Liu, C. Cui, H. Ren, M. Gu, H. Liu, Z. Zhou and F. Qi, *Fuel*, 2024, **361**, 130719.
69 Q. Wang, X. Zhang, S. Sun, Z. Wang and D. Cui, *ACS Omega*, 2020, **5**, 10276–10287.
70 X. Liu, Y. Wu, J. Zhang, Y. Zhang, X. Li, H. Xia and F. Wang, *ACS Omega*, 2022, **7**, 18953–18968.
71 Y.-K. Park, J. Jung, S. Ryu, H. W. Lee, M. Z. Siddiqui, J. Jae, A. Watanabe and Y.-M. Kim, *Appl. Energy*, 2019, **250**, 1706–1718.